ADVANCED FUNCTIONAL MATERIALS
www.afm-journal.de

A Flexible and Regenerative Aptameric Graphene–Nafion Biosensor for Cytokine Storm Biomarker Monitoring in Undiluted Biofluids toward Wearable Applications

Ziran Wang, Zhuang Hao, Xuejun Wang, Cong Huang, Qiao Lin, Xuezeng Zhao, and Yunlu Pan**

Wearable sensors that can conveniently detect cytokine levels in human biofluids are essential for assisting hospitals to maximize the benefits of anti-inflammatory therapies and avoid cytokine storms. Measurement of cytokine levels in biofluids still remains challenging for existing sensors due to high interference from the background. Here, this challenge is overcome through developing a flexible and regenerative aptameric field-effect transistor biosensor, consisting of a graphene–Nafion composite film, for detecting cytokine storm biomarkers in undiluted human biofluids. The composite film enables the minimization of nonspecific adsorption and empowers the renewability to the biosensor. With these capabilities, the device is capable of consistently and sensitively monitoring cytokines (e.g., IFN-γ, an inflammatory and cancer biomarker) in undiluted human sweat with a detection range from 0.015 to 250 nM and limit of detection down to 740 fM. The biosensor is also shown to incur no visible mechanical damage and maintain a consistent sensing response throughout the regenerative (up to 80 cycles) and crumpling (up to 100 cycles) tests. Experimental results demonstrate that the biosensor is expected to offer opportunities for developing wearable biosensing systems for distinguishing acute infectious disease patients and monitoring of patients' health conditions in daily life.

1. Introduction

As an essential response of the immune system against diseases, inflammation is able to eliminate infectious agents.[1,2] However, certain diseases such as coronavirus disease 2019 (COVID-19), severe acute respiratory syndrome, and ebola virus disease may lead to excessive and prolonged inflammation response known as "cytokine storm", which would result in higher mortality since it could cause severe damage to human organs, acute respiratory distress syndrome, or sudden deterioration of the patient's condition.[3–5] In the meanwhile, cytokines are also critical biomarkers for trauma, sepsis, cancers, and rheumatic diseases.[6,7] Thus, it is highly desirable to develop a kind of point-of-care wearable sensors for continuous detection of patients' cytokine levels, which could not only distinguish acute infectious disease patients who are worsening but also monitor health conditions in daily life.

Conventional cytokine detection methods such as immunofluorescence and enzyme-linked immunosorbent assay,[8,9] which are time-consuming and require bulky instruments and complicated operations, would be difficult to employ in wearable sensors. Miniature detection devices (e.g., electrochemical sensors) have focused on reducing sensor response time and improving sensing accuracy in the face of cytokines in high ionic strength buffers such as phosphate buffer.[10,11] However, most of these sensors still have limited capability for realizing cytokine detection in physiologically relevant environments, especially for wearable applications, due to the low cytokine concentration and background interferences in human biofluids (e.g., sweat, tears, and saliva).[12–14] Therefore, developing wearable sensors, which can enable sensitive and continuous detection of cytokines in undiluted human biofluids, are of great significance for conveniently monitoring patients' disease conditions in daily life.

Recently, due to the unique electronic and chemical properties such as high carrier mobility, sensitivity to molecules and good biocompatibility,[15–17] graphene, a 2D carbon material with sp^2 structure, has aroused significant amounts of attention for biomarker detection using graphene-based biosensors.[18–20] Such devices have been used to detect metabolites[21,22] (e.g., glucose

Z. Wang, Dr. Z. Hao, C. Huang, Prof. X. Zhao, Prof. Y. Pan
School of Mechatronics Engineering
Harbin Institute of Technology
Harbin 150001, China
E-mail: haozhuang@hit.edu.cn; yunlupan@hit.edu.cn
Z. Wang, Dr. Z. Hao, C. Huang, Prof. X. Zhao, Prof. Y. Pan
Key Laboratory of Micro-systems and Micro-structures Manufacturing
Ministry of Education
Harbin Institute of Technology
Harbin 150080, China
Dr. Z. Hao
School of Chemistry and Chemical Engineering
Harbin Institute of Technology
Harbin 150001, China
Dr. X. Wang
State Key Laboratory of Molecular Engineering of Polymers
Fudan University
Shanghai 200433, China
Prof. Q. Lin
Department of Mechanical Engineering
Columbia University
New York, NY 10027, USA
The ORCID identification number(s) for the author(s) of this article can be found under https://doi.org/10.1002/adfm.202005958.

DOI: 10.1002/adfm.202005958

and lactate) and simple ions[23,24] (e.g., Na^+ and Ca^{2+}) in human biofluids. To recognize more complex biomarkers (e.g., proteins), graphene-based affinity biosensors have been developed by using aptamers or antibodies as detection probes,[25,26] which are capable of binding various biomarkers with high affinity and specificity. However, most of these biosensors can only realize detection in heavily diluted human biofluids (more than 100 times),[27–29] due to the highly nonspecific adsorption of complex components in biofluids and the limited sensor sensitivity.[30]

This paper develops a flexible and regenerative aptameric graphene–Nafion field-effect transistor (GNFET) biosensor that is capable of sensitively and consistently detecting cytokine storm biomarkers in undiluted human biofluids. The graphene–Nafion composite film offers the effective elimination of the interferences from nonspecific adsorption, and empowers the capability of regeneration to the graphene field-effect transistor, as the biosensors sensitively detect biomarkers in undiluted biofluids (e.g., human sweat was used as a representative) and regenerate up to 80 times without electrical and mechanical failure. In addition, thanks to the flexibility and durability of the graphene–Nafion composite film, the device is capable of conforming to underly surfaces (e.g., human hand and wrist), or withstanding cyclic crumpling tests (up to 100 cycles). Experimental results demonstrate the biosensor maintains the highly consistent and sensitive detection of IFN-γ, a representative inflammatory cytokine biomarker, in undiluted human sweat under different conditions, with a detection range from 0.015 to 250 nM and limit of detection (LOD) down to 740 fM. Considering these results, the biosensor could potentially be used in daily noninvasive cytokine detection in human sweat and other biofluids in wearable applications.

2. Results and Discussion

The GNFET biosensor consists of a graphene–Nafion composite film as a conducting channel, which can consistently and sensitively detect cytokine biomarkers in undiluted human biofluids (**Figure 1**a). Nafion is a fluoropolymer, consisting

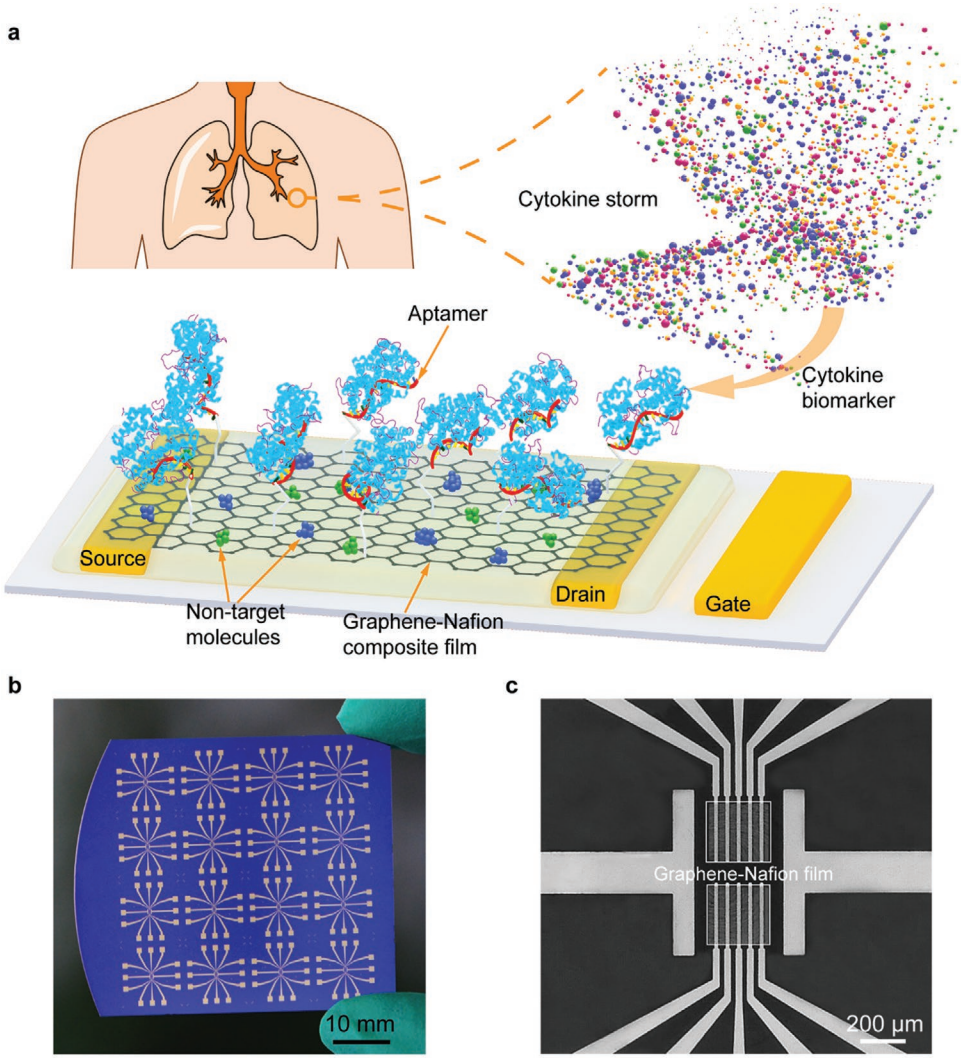

Figure 1. Graphene–Nafion field-effect transistor (GNFET) biosensor device. a) Schematic of the aptameric GNFET biosensor for cytokine biomarker detection. b) Photograph of the large-scale fabricated biosensor. c) Microscope image of a GNFET biosensor.

of tetrafluoroethylene backbone incorporated perfluorovinyl ether groups terminated with sulfonate groups. The abundant fluorocarbon and sulfonic acid groups enable the film to possess high chemical resistance, mechanical stability, and great permeability to cations.[31–33] The composition of the film was verified through the energy dispersive spectroscopy (EDS) and X-ray photoelectron spectroscopy (XPS) (Figure S1, Supporting Information). Hence, Nafion not only can (1) prevent the graphene and electrodes contacting with interferences in the solution, but also (2) anchor aptamer probes that can recognize and capture the specific biomarker via chemical bond. A drain–source bias is applied to the conducting channel with an electrical double layer (EDL) generated at the interface of the graphene–Nafion composite film and the electrolyte serving as the gate dielectric. The change in the drain–source current arising from the aptamer–biomarker interaction is measured to determine the biomarker concentration. Figure 1b shows a photograph of the large-scale fabricated biosensor array with a size of 4 cm × 4 cm. A microscope image shows that the Nafion film has completely covered the graphene surface (Figure 1c), effectively suppressing the nonspecific adsorption occurred on the sensor surface. In addition, surface parameters of the graphene–Nafion composite film were characterized using atomic force microscope, with the thickness about 51.7 ± 2.58 nm and the surface roughness, around 4.2 ± 0.46 nm (Figure S2, Supporting Information).

FETs are fabricated according to our previously reported fabrication protocols,[34,35] while the graphene–Nafion composite film, which offers the regenerative capability to the biosensor, is developed as a conducting channel for the first time (**Figure 2**a). First, metal electrodes (45 nm of Cr/Au) were fabricated using the standard photolithography technique, e-beam deposition, and lift-off photoresist removal. Then, the monolayer graphene that synthesized by chemical vapor deposition (CVD) was transferred onto electrodes. Subsequently, Nafion solution was dropped cast on the graphene surface to form an isolated layer. Finally, graphene–Nafion composite film was functionalized with aptamers specific to the biomarker. After each cycle of the biomarker detection, the GNFET biosensor was immersed in ethanol solution to dissolve the Nafion film, hence obtaining a brand new graphene-based FET that can be regenerated and reused for the next biomarker detection cycle. A microscopy image of the graphene-based biosensor was shown in Figure 2b, with a zoom-in scanning electron microscope (SEM) image of the graphene shown in the inset.

Detection of the biomarker is enabled by the interaction between the specific aptamer and target biomarker. The abundant sulfonate head groups in the Nafion film were used as linkers to anchor aptamers. Ethanolamine was then applied to quench unreacted sulfonate head groups in the Nafion film. Functionalization of the biosensor was verified by investigating electrical properties of the graphene. As shown in Figure 2c, the Dirac point (V_{Dirac}), the gate voltage (V_{g}) at which the drain–source current (I_{ds}) reaches its minimum, is observed to be increased from 0.176 to 0.336 V after the Nafion film coated the graphene surface. After the attachment of aptamer, V_{Dirac} decreases to 0.193 V, indicating that the n-type doping is induced to the conducting channel. Further, EDS was employed to characterize the sulfonate head groups in the Nafion film and the aptamer functionalization (Figure 2d). Elements of sulfur and phosphorus are observed to considerably exist on the conducting channel, which are the unique constituent elements of the sulfonate head groups and aptamer, respectively. These results illustrate the successful functionalization of the GNFET biosensor using the graphene–Nafion composite film and aptamer.

The biomarker detection's capability for the GNFET biosensor was first tested in 150 mM phosphate buffer saline (1×PBS) (**Figure 3**a). Values of the response signal to the biomarker concentration changes were used as a baseline of comparison for assessing devices' performance in human biofluids. IFN-γ, which is an inflammatory cytokine closely related to inflammation, COVID-19, and cancers, was used as a representative.[36] A polydimethylsiloxane well was mounted on the device to handle the analyte solution. In the tests, V_{g} was swept from 0 to 0.3 V at a step of 0.002 V with the drain–source voltage, V_{ds}, fixed at 0.03 V. As the concentration of IFN-γ increases from 0.015 to 250 nM, V_{Dirac} decreases by 0.027 V from 0.193 to 0.166 V (Figure 3b). Induction of n-type doping to graphene via electrostatic gating effect could potentially explain the shift in V_{Dirac}.[37,38] In the absence of IFN-γ, the aptamer that immobilized on the graphene surface is in a flexible, loop, and unfolded state. Upon binding with IFN-γ, the aptamer switches to a stable and compact conformation. Thereby, the negatively charged aptamer together with negatively charged IFN-γ is brought into the close vicinity of graphene–Nafion composite film, altering the charge distribution in EDL and resulting in charge changes in the graphene due to electrostatic induction,[27,39] and hence generating a detectable change in the measured I_{ds}.

To study the binding affinity between aptamer and IFN-γ, the equilibrium dissociation constant (K_{D}) was investigated. During tests, the shift in V_{Dirac}, denoted $\Delta V_{\mathrm{Dirac}} = V_{\mathrm{Dirac}} - V_{\mathrm{Dirac,0}}$ ($V_{\mathrm{Dirac,0}}$ is the value corresponding to the solution without target biomarkers), is normalized to eliminate the effect of device-to-device non-uniformities resulted from the fabrication process and material properties. The normalized $\Delta V_{\mathrm{Dirac}}$ is defined as $\Delta V_{\mathrm{Dirac}}/\Delta V_{\mathrm{Dirac,max}}$, where $\Delta V_{\mathrm{Dirac,max}} = V_{\mathrm{Dirac,max}} - V_{\mathrm{Dirac,0}}$ with $V_{\mathrm{Dirac,max}}$ the Dirac point corresponding to the maximum IFN-γ concentration. As shown in Figure 3c, the affinity between aptamer and IFN-γ can be calculated using the Hill–Langmuir model,[18]

$$\frac{\Delta V_{\mathrm{Dirac}}}{\Delta V_{\mathrm{Dirac,max}}} = A\frac{(C_{\mathrm{IFN}}/K_{\mathrm{D}})^n}{1+(C_{\mathrm{IFN}}/K_{\mathrm{D}})^n} \quad (1)$$

where A is the saturation response coefficient of the biosensor, C_{IFN} is the concentration of IFN-γ protein, and n is the Hill coefficient reflecting the binding cooperativity. In accordance with the fitted curve, K_{D} is estimated to be 4.39 nM, indicating the strong binding tendency between aptamer and IFN-γ. These results compared favorably with the existing sensors for IFN-γ detection.[40]

The specificity of the biosensor was examined using control protein molecules, TNF-α, interleukin-002 (IL-002), and interleuk-6 (IL-6), which are closely related inflammatory cytokines to IFN-γ. The biosensor was exposed to different concentrations of control proteins in 1×PBS under the same measurement condition in IFN-γ detection. It can be seen the normalized

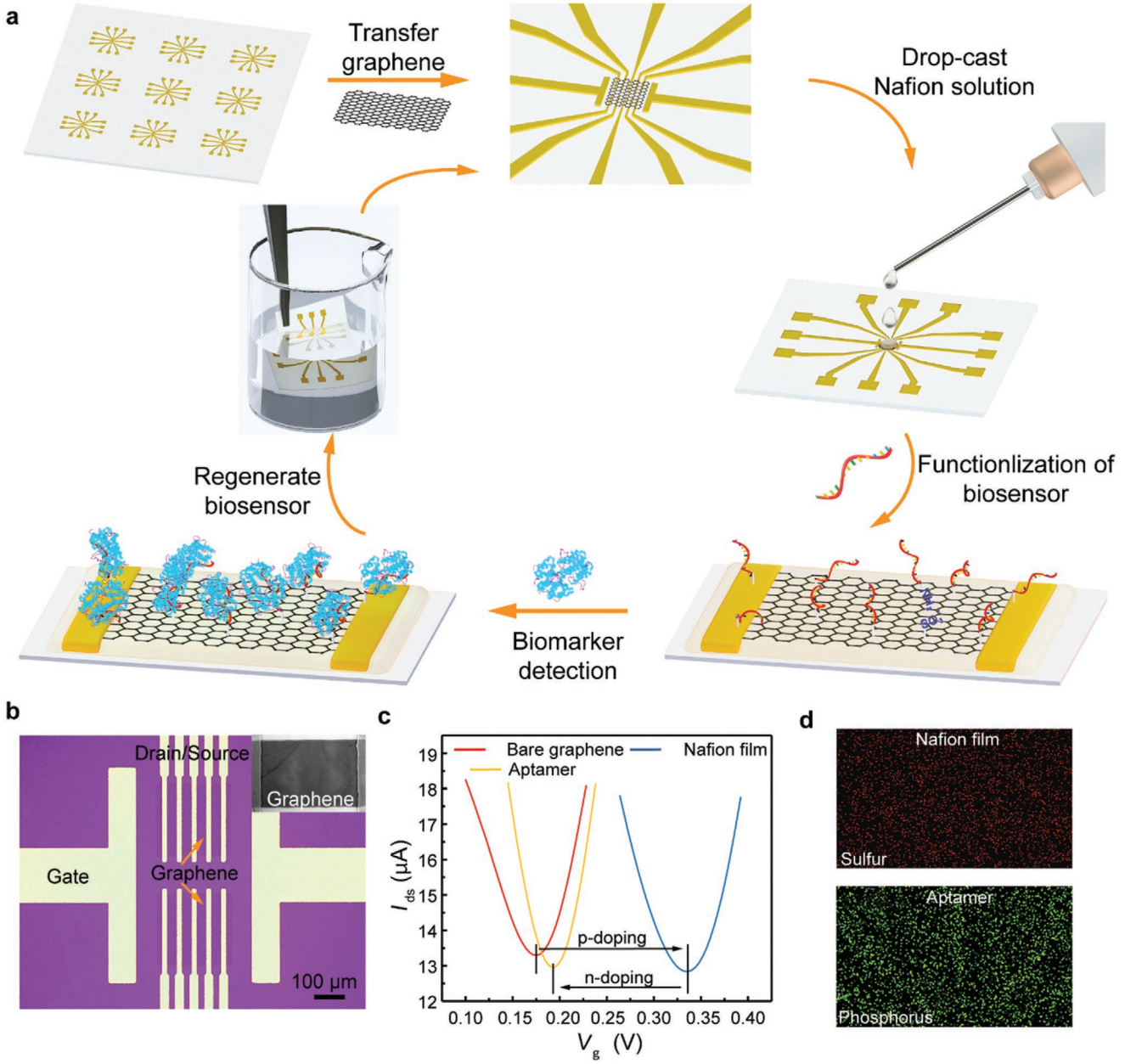

Figure 2. Fabrication and biochemical functionalization of the biosensor. a) Illustration of the fabrication, detection, and regenerative process of the GNFET biosensor. b) Microscope image of the fabricated device with graphene and on-chip electrodes. c) Transfer characteristic curves of the biosensor before and after Nafion and aptamer modification. d) EDS shows that the sulfur exists on the Nafion film, and phosphorus is widely coated on the biosensor after aptamer modification.

signal $\Delta V_{Dirac}/\Delta V_{Dirac,max}$ for IFN-γ is more than five times larger than those for the control proteins at the same concentration (Figure 3d), illustrating that the GNFET biosensor possessed the high specificity to the target biomarker.

In order to better investigate the applicability of the GNFET biosensor in real-life scenarios, the human sweat, which is easily collected and contains numerous cytokine biomarkers, was chosen as the representative sample to conduct biomarker detection. The GNFET biosensor was first tested in undiluted artificial sweat, which contains consistent ingredients as human sweat such as NaCl, KCl, urea, lactic acid, and amino acids.[41] As the IFN-γ concentration increases from 0.015 to 250 nM, the transfer characteristic curve shifts to negative direction consistently with a maximum ΔV_{Dirac} value of 0.028 V (**Figure 4**a). Compared with the value obtained in 1×PBS (0.027 V), the difference is less than 3.7%. Also, the K_D is calculated to be 4.28 nM (Figure 4b), which is consistent with the value obtained in 1×PBS (4.39 nM). Hence, the response of the GNFET biosensor for the biomarker detection remains highly consistent and reliable in artificial sweat.

Time-resolved measurement of IFN-γ concentration in undiluted artificial sweat was subsequently carried out. In tests, V_{ds} and V_g were fixed at 0.03 and 0.2 V, respectively. The change

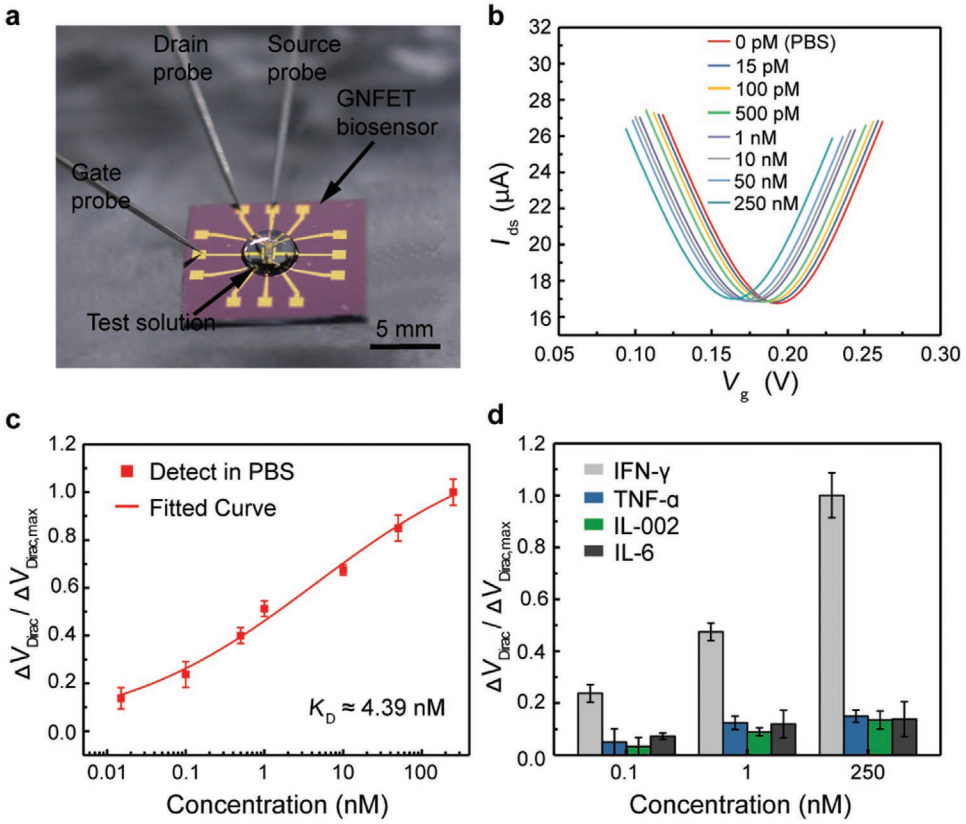

Figure 3. Biomarker detection in PBS. a) Photograph of the GNFET biosensor for biomarker detection. b) Transfer characteristic curves measured when the device was exposed to IFN-γ solution ranging from 0 to 250 nM in PBS. c) Normalized Dirac point shift $\Delta V_{Dirac}/\Delta V_{Dirac,max}$ as a function of IFN-γ concentrations. The red line is a least-square fit to the Hill-Langmuir binding model. d) Sensing response of the biosensor to IFN-γ and control proteins (TNF-α, IL-002, and IL-6) with different concentrations (0.1, 1, and 250 nM).

in I_{ds} is denoted as $\Delta I_{ds} = I_{ds} - I_{ds,0}$ ($I_{ds,0}$ is the value measured in the solution without biomarkers), and the normalized I_{ds} is defined as $\Delta I_{ds}/\Delta I_{ds,max}$, where $\Delta I_{ds,max}$ is the maximum value of ΔI_{ds}. As shown in Figure 4c, the stepwise and dramatic increase from 0 to 0.98 in $\Delta I_{ds}/\Delta I_{ds,max}$ is observed with the biosensor exposure to IFN-γ solutions at concentrations ranging from 0.015 to 50 nM. Further, the binding interaction between aptamer and IFN-γ is observed to reach equilibrium within 6 min.

To study the potential capability of the biosensor for consistent and sensitive detection of biomarkers in undiluted human biofluids for monitoring the physiologic state of humans in daily life, the biomarker detection in undiluted human sweat was carried out. Human sweat was collected from healthy volunteers using sweat collection capsules (**Figure 5**a) (see Experimental Section for details). Compared with 1×PBS and artificial sweat, the human sweat contains abundant

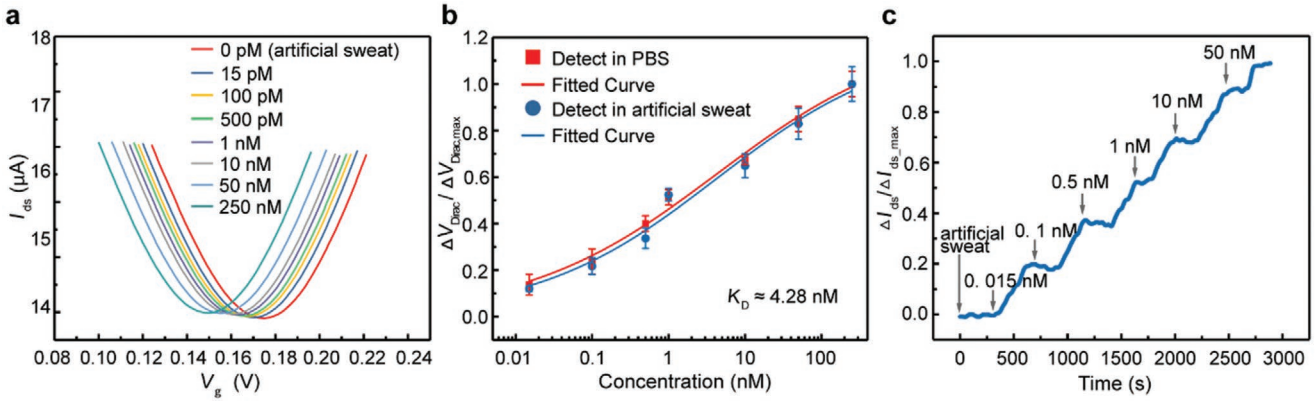

Figure 4. Biomarker detection in artificial sweat. a) Transfer characteristic curves measured when GNFET biosensor was exposed to different IFN-γ concentrations in undiluted artificial sweat. b) Normalized $\Delta V_{Dirac}/\Delta V_{Dirac,max}$ as a function of various IFN-γ concentrations in PBS (square) and artificial sweat (circle). c) Time-resolved measurement of changes in IFN-γ concentrations in artificial sweat.

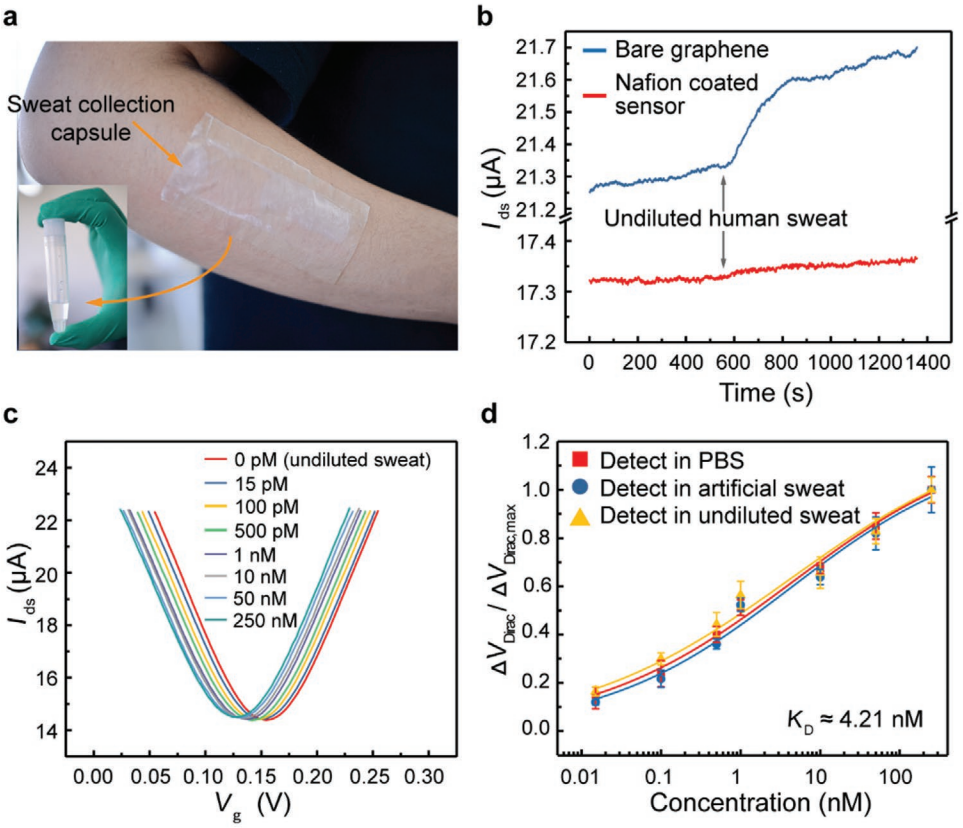

Figure 5. Biomarker detection in undiluted human sweat. a) Photograph of the process of the human sweat collection b) Time-resolved measurement of bare graphene sensor (blue line) and Nafion film coated sensor (red line) represent that the nonspecific binding in sweat is minimized with the existence of Nafion film. c) Transfer characteristic curves measured when the biosensor was exposed to various IFN-γ concentrations in undiluted sweat. d) Normalized $\Delta V_{Dirac}/\Delta V_{Dirac,max}$ as a function of different IFN-γ concentrations in PBS (square), artificial sweat (circle), and undiluted sweat (triangle).

nontarget molecules that would cause nonspecific adsorption on the conducting channel. To overcome this problem, a porous and negatively charged Nafion film was used to completely isolate graphene from the solution and screen out nontarget molecules (e.g., lactic acid and amino acids) that may disturb the biomarker sensing. Time-resolved signals of the traditional graphene-based FET and our novel graphene–Nafion FET exposed to the human sweat are shown in Figure 5b. The measured I_{ds} of traditional graphene-based FET exhibits a dramatic increase (≈0.3 μA) upon exposure to the sweat, while no significant change is observed in I_{ds} from graphene–Nafion FET, demonstrating that the nonspecific adsorption of nontarget molecules on the conducting channel has been largely suppressed by the Nafion film.

The biomarker detection in undiluted human sweat was then investigated (Figure 5c). As the IFN-γ concentration increases from 0.015 to 250 nM, the sensor response maintains a high consistency with values measured in 1×PBS. The maximum ΔV_{Dirac} is 0.026 V with a variation less than 3.7% compared with the ΔV_{Dirac} measured in 1×PBS (0.027 V). The sensing signal detected in undiluted sweat holds a high level of consistency with that tested in 1×PBS and artificial sweat (Figure 5d). The K_D obtained in human sweat is estimated to be 4.21 nM, differing from the value estimated in 1×PBS (4.39 nM) or artificial sweat (4.28 nM) by less than 4.2%. The LOD for IFN-γ detection is estimated to be 740 fM, which is tens of times lower than LOD obtained using existing methods.[42,43] The enhance of these sensing responses are attributed to the graphene surface covered with Nafion film, which effectively suppresses the adsorption of human sweat nontarget interferences onto the biosensor. It can be concluded that the response of our device affords a high consistency and sensitivity in biomarker detection in human sweat.

In addition to the consistent and specific detection of biomarkers in different physiological solutions, it is also expected that the biosensor can be reusable and have extended service life in practical applications. Traditionally, the graphene conducting channel is directly functionalized with aptamers or other probes (e.g., enzyme and antibody) through irreversible chemical bonding.[25,44] However, these methods cannot remove the aptamer, which has bound to the biomarker, from the graphene surface, thus impeding the biosensor to be cyclically used. As a proof-of-concept, we demonstrate the GNFET biosensor with the capability for multiple regenerative cycles, where the consistent and sensitive detection of the biomarker can be maintained. The mechanical integrity of the graphene throughout the regenerative cycles was characterized (**Figure 6**a). No visible mechanical damages on the graphene are observed, and the Nafion film is completely removed without residues. XPS was utilized to further verify that no residues of the Nafion film were adsorbed

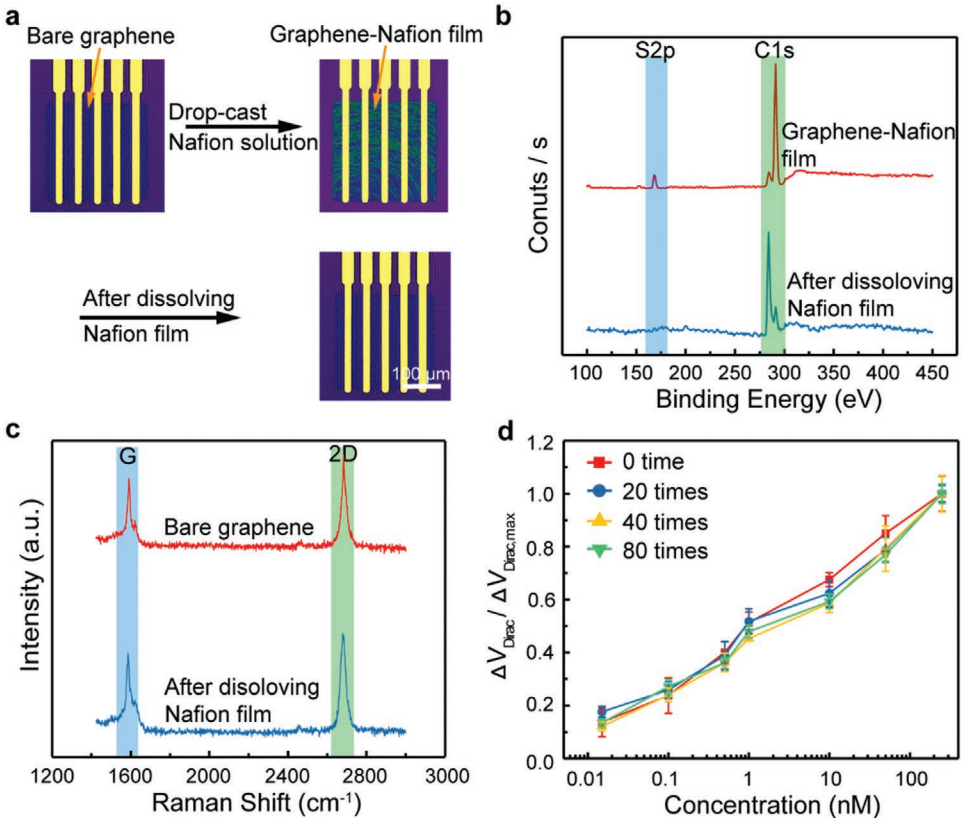

Figure 6. Characterization of the regenerative biosensor. a) Microscope image showing the regenerative process of the biosensor. b) XPS showing the peak of the sulfur element on the graphene–Nafion film and after dissolving Nafion film. c) Raman spectra of the graphene before and after dissolving the Nafion film. d) Detection of IFN-γ with concentrations ranging from 0.015 to 250 nM using the biosensor with different regenerative cycles.

on the graphene (Figure 6b). Compared with the graphene–Nafion film, the peak of sulfur element is negligible after dissolving the Nafion film. Properties of graphene after removing the Nafion film was verified using Raman spectra (Figure 6c). Positions of G-band and D-band show the high consistency with that obtained on the bare graphene, which illustrates that the dissolution of Nafion film has an inappreciable effect on the graphene's electrical properties. After multiple regenerative cycles, the biosensor was subsequently tested for the IFN-γ detection (Figure 6d). The sensor response is consistent with the signal values obtained in the first cycle at the same concentration; with a variation less than 8.3% (see Figure S3, Supporting Information, for transfer characteristic curves). This suggests that the GNFET biosensor possesses the capability of the consistent and sensitive detection of the biomarker after reuse and reconstruction for multiple cycles.

We also preliminarily present a flexible and robust GNFET biosensor that fabricated on an ultrathin polyethylene terephthalate film (6 μm) toward wearable applications. As shown in **Figure 7**a, the biosensor is observed to be highly flexible and capable of conformably mounting onto practically relevant support such as human hands. The device was mounted on the artificial human hand to evaluate the capability of IFN-γ measurement in human sweat (Figure 7b). The sensing response holds a high level of consistency with that obtained in prior experiments. The maximum ΔV_{Dirac} is 0.025 V, whose deviation from the ΔV_{Dirac} value measured on the sensor fabricated on wafer (0.026 V) is less than 3.8%. The K_D is calculated to be 4.23 nM, which is consistent with the value of K_D measured on the sensor fabricated on wafer (4.21 nM), and the LOD is estimated to be 880 fM (see Figure S4, Supporting Information, for transfer characteristic curves). In order to further characterize the flexibility and robustness of the biosensor, crumpling experiments were carried out. The ultrathin biosensor foil was severely crumpled from its original size as a small ball and then flattened (Figure 7c). No visible mechanical damage is observed throughout the crumpling tests. The IFN-γ detection of the biosensor that undergoes multiple crumpling cycles was shown in Figure 7d. The sensor response to IFN-γ is highly consistent with that tested before crumpling, with variation less than 3.6% at the same concentration. The maximum ΔV_{Dirac} is 28.8 mV (100 crumpling cycles), and the deviation is less than 4.1% throughout the crumpling tests (see Figure S5, Supporting Information, for transfer characteristic curves). Results show that the GNFET biosensor offers a high degree of flexibility and robustness and hence can be potentially deployed on human body for consistent monitoring of disease biomarkers.

3. Conclusion

In summary, we developed a flexible and regenerative affinity-based GNFET biosensor that enables the consistent,

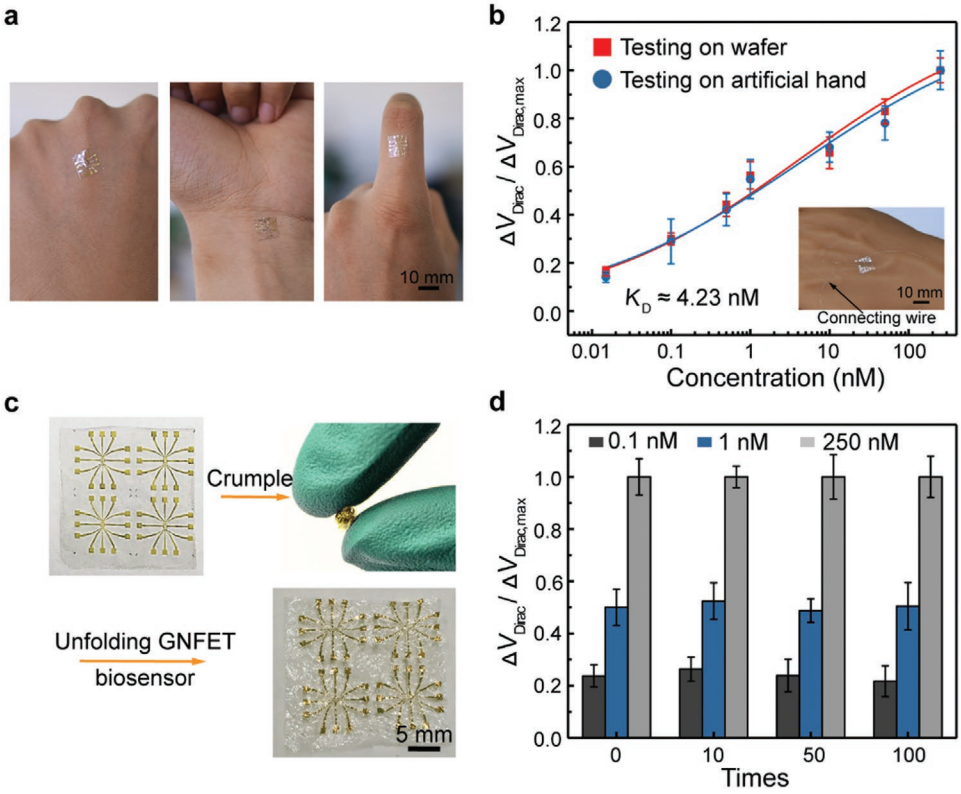

Figure 7. Characterization of the highly flexible biosensor. a) Photograph of the highly flexible biosensor conformably mounted on the human hand. b) Normalized Dirac point shift $\Delta V_{Dirac}/\Delta V_{Dirac,max}$ showing the sensing response to the biomarker in undiluted human sweat using the flexible device placed on the artificial hand. c) Photograph of the crumping process of the biosensor. d) Sensing response of the biosensor to various IFN-γ concentrations (0.1, 1, and 250 nM) at different crumpling cycles.

sensitive, and specific detection of cytokine storm biomarkers in undiluted human biofluids toward wearable application. The biosensor configures with a monolayer graphene sheet that is overlaid by a chemically inert Nafion film as the conducting channel. The graphene–Nafion film is modified with the aptamer specific to the biomarker. The specific binding between aptamer and biomarker induced a change in the carrier concentration, which is detected to determine the biomarker concentration. The biosensor possesses a high level of consistency and sensitivity for biomarker detection in undiluted human sweat, as well as the capability for achieving multiple regenerative cycles (up to 80 cycles), or withstanding cyclic crumpling tests (up to 100 cycles) without mechanical failure. In experiments, the biosensor was capable of sensitive monitoring of IFN-γ in 1×PBS, artificial sweat, and undiluted human sweat, with the LOD down to 740 fM, and variations in the signal value less than 6.8% at the same concentration. Moreover, no visible mechanical damage could be observed throughout the cyclic regenerative and crumpling tests, and the sensing response maintains highly consistent with first time tested results. The flexible biosensor is also capable of conformably mounting on various supports to consistently detect IFN-γ in undiluted human sweat, with the LOD down to 880 fM. We propose that our biosensor would offer opportunities for convenient and rapid monitoring of COVID-19 in human biofluids using the biosensor modified with probes specific to its biomarker. Such biosensor has the potential to play a critical role in providing rapid information of patients' condition with acute infectious diseases, and helping hospitals stratify COVID-19 patients according to disease severity.

4. Experimental Section

Materials: Monolayer CVD graphene was ordered from Graphenea (Cambridge, MA). 285 nm SiO_2/Si wafer was purchased from UniversityWafer (Boston, MA). Polyethylene terephthalate film (6 µm) was ordered from Chemplex Industries (Florida, USA). 1-Pyrenebutyric acid *N*-hydroxysuccinimide ester, Nafion solution, ethanolamine, human IL-6, and human IL-002 were purchased from Sigma-Aldrich (St. Louis, MO). Phosphate buffered saline (1×PBS, pH = 7.4) was ordered from Thermo Fisher Scientific (Massachusetts, USA). TNF-α and IFN-γ proteins were ordered from R&D Systems (Minneapolis, MN). IFN-γspecific aptamer (5′-NH_2- GGG GTT GTT TGT GTT GGG TGT TGT GT -3′) was synthesized and purified by Sangon Biotech (Shanghai, China). The artificial sweat was ordered from Pickering Laboratories (California, USA).

Biosensor Fabrication: The biosensor was fabricated following the authors' previous fabrication protocol. The photoresist was first spin-coated on the 285 nm SiO_2/Si wafer that was cleaned with acetone. Upon the process of exposure and developing, the electrodes (2 nm Cr/43 nm Au) were deposited on the wafer using the standard metal deposition techniques. Finally, the photoresist was released by dipping the chip in acetone with ultrasound for 5 min at room temperature. To transfer the graphene onto the biosensor, the device was first exposed to the oxygen plasma to clean the surface and increase the surface

hydrophilicity. The synthesized graphene was then transferred onto the substrate using the wet floating-transfer method.

Biochemical Functionalization: 5 µL of 0.1 wt% Nafion solution was first drop cast on the graphene surface to form a complete isolated layer, and then the biosensor was heated at 80 °C for 5 min. Subsequently, the device was incubated in the PBS solution with 5 µM IFN-γ-specific aptamer overnight at room temperature. After washing with PBS, the biosensor was immersed in 100 mM ethanolamine solution for 20 min to block the unreacted sulfonate head groups on the Nafion film.

Human Sweat Collection: Human sweat samples were collected from healthy volunteers (1#: male, 25 years, 2#: male, 28 years, and 3#: male, 30 years) according to previously reported collection procedure.[34,35] Briefly, the sweat sampling was performed using a sweat collection capsule, which consists of an adhesive and disposable membrane being attached to the forehead and forearm with a fluid-tight window that was given access to collect sweat. The volunteers were asked to exercise 20 min under the same condition. The collected sweat samples were spiked with different IFN-γ concentrations and stored at 4 °C before testing.

Characterization: Microscope images were obtained using Lecia Digital Microscope DVM6, and SEM images were taken with FEI Quanta 200FEG-SEM. The Raman spectra were tested using Renishaw inVia micro-Raman, excitation laser wavelength 532 nm. The device's electrical properties and transfer curves were characterized by Keiteley 2636B sourcemeters.

Supporting Information

Supporting Information is available from the Wiley Online Library or from the author.

Acknowledgements

The authors thank L. Liu for their contribution as a participant in the experiments involving human sweat collection. This work is supported by the National Institutes of Health (Grant No. 1DP3DK101085-01 and 1R33CA196470-01A1), the National Science Foundation (Grant No. ECCS-1509760), the National Natural Science Foundation of China (Grant Nos. 51975145), the China Postdoctoral Science Foundation (Grant Nos. 2019M661270), the Heilongjiang Postdoctoral Science Foundation (Grant Nos. LBH-Z19221) and the National Postdoctoral Program for Innovative Talents (Grant No. BX20200105). Informed consent was obtained from the participants (Z. Wang, Z. Hao and L. Liu) for sweat collection and tests performed with the fabricated sensor on their skin.

Conflict of Interest

The authors declare no conflict of interest.

Keywords

cytokine storm biomarkers, graphene–Nafion composite films, human biofluids, wearable biosensors

Received: July 15, 2020
Revised: September 7, 2020
Published online:

[1] Y. Yang, C. Shen, J. Li, J. Yuan, M. Yang, F. Wang, G. Li, Y. Li, L. Xing, L. Peng, J. Wei, M. Cao, H. Zheng, W. Wu, R. Zou, D. Li, Z. Xu, H. Wang, M. Zhang, Z. Zhang, L. Liu, Y. Liu, *medRxiv* **2020**, https://doi.org/10.1101/2020.03.02.20029975.
[2] R. Channappanavar, S. Perlman, *Semin. Immunopathol.* **2017**, *39*, 529.
[3] M. Kermali, R. K. Khalsa, K. Pillai, Z. Ismail, A. Harky, *Life Sci.* **2020**, *254*, 117788.
[4] C. Huang, Y. Wang, X. Li, L. Ren, J. Zhao, Y. Hu, L. Zhang, G. Fan, J. Xu, X. Gu, Z. Cheng, T. Yu, J. Xia, Y. Wei, W. Wu, X. Xie, W. Yin, H. Li, M. Liu, Y. Xiao, H. Gao, L. Guo, J. Xie, G. Wang, R. Jiang, Z. Gao, Q. Jin, J. Wang, B. Cao, *Lancet* **2020**, *395*, 497.
[5] S. M. Russell, A. Alba-Patiño, E. Barón, M. Borges, M. Gonzalez-Freire, R. de la Rica, *ACS Sens.* **2020**, *5*, 1506.
[6] S. Lukasiak, C. Schiller, P. Oehlschlaeger, G. Schmidtke, P. Krause, D. F. Legler, F. Autschbach, P. Schirmacher, K. Breuhahn, M. Groettrup, *Oncogene* **2008**, *27*, 6068.
[7] C. I. Westacott, J. T. Whicher, I. C. Barnes, D. Thompson, A. J. Swan, P. A. Dieppe, *Ann. Rheum. Dis.* **1990**, *49*, 676.
[8] C. Lam, M. A. Pavel, P. Kashyap, Z. Salehi-Najafabadi, V. Valentino, Y. Yu, in *Cytokine Bioassays: Methods and Protocols*, 1st ed. (Ed: I. Vancurova) Springer, New York **2014**, p. 193.
[9] G. Shankar, D. A. Cohen, *J. Immunoassay* **1997**, *18*, 371.
[10] Y. Chen, T. S. Pui, P. Kongsuphol, K. C. Tang, S. K. Arya, *Biosens. Bioelectron.* **2014**, *53*, 257.
[11] H. Zhang, B. Jiang, Y. Xiang, Y. Chai, R. Yuan, *Analyst* **2012**, *137*, 1020.
[12] J. Heikenfeld, *Electroanalysis* **2016**, *28*, 1242.
[13] C. J. Harvey, R. F. LeBouf, A. B. Stefaniak, *Toxicol. In Vitro* **2010**, *24*, 1790.
[14] W. A. Skinner, H. Tong, H. Johnson, H. Maibach, D. Skidmore, *Experientia* **1968**, *24*, 679.
[15] B. J. Kim, H. Jang, S. K. Lee, B. H. Hong, J. H. Ahn, J. H. Cho, *Nano Lett.* **2010**, *10*, 3464.
[16] A. K. Geim, K. S. Novoselov, *Nat. Mater.* **2009**, *6*, 11.
[17] D. Choi, M.-Y. Choi, W. M. Choi, H.-J. Shin, H.-K. Park, J.-S. Seo, J. Park, S.-M. Yoon, S. J. Chae, Y. H. Lee, *Adv. Mater.* **2010**, *22*, 2187.
[18] Y. Ohno, K. Maehashi, K. Matsumoto, *J. Am. Chem. Soc.* **2010**, *132*, 18012.
[19] Y. Song, Y. Luo, C. Zhu, H. Li, Y. Lin, *Biosens. Bioelectron.* **2015**, *76*, 195.
[20] Y. Shao, J. Wang, H. Wu, J. Liu, I. A. Aksay, Y. Lin, *Electroanalysis* **2010**, *22*, 1027.
[21] J. Kim, M. Kim, M.-S. Lee, K. Kim, S. Ji, Y.-T. Kim, J. Park, K. Na, K.-H. Bae, H. K. Kim, F. Bien, C. Y. Lee, J.-U. Park, *Nat. Commun.* **2017**, *8*, 14997.
[22] C. Xiong, T. Zhang, W. Kong, Z. Zhang, H. Qu, W. Chen, Y. Wang, L. Zheng, *Biosens. Bioelectron.* **2018**, *101*, 21.
[23] Q. B. An, S. Y. Gan, J. N. Xu, Y. Bao, T. S. Wu, H. J. Kong, L. J. Zhong, Y. M. Ma, Z. Q. Song, L. Niu, *Electrochem. Commun.* **2019**, *107*, 106553.
[24] G. Xu, C. Cheng, W. Yuan, Z. Y. Liu, L. H. Zhu, X. T. Li, Y. L. Lu, Z. T. Chen, J. L. Liu, Z. Cui, J. J. Liu, H. Men, Q. J. Liu, *Sens. Actuators B* **2019**, *297*, 126743.
[25] Z. Hao, Y. Zhu, X. Wang, P. Rotti, C. Dimarco, S. Tyler, X. Zhao, J. F. Engelhardt, J. C. Hone, Q. Lin, *ACS Appl. Mater. Interfaces* **2017**, *9*, 27504.
[26] Z. Wang, Z. Hao, S. Yu, C. G. D. Moraes, L. H. Suh, X. Zhao, Q. Lin, *Adv. Funct. Mater.* **2019**, *29*, 1905202.
[27] Z. Hao, Y. Pan, W. Shao, Q. Lin, X. Zhao, *Biosens. Bioelectron.* **2019**, *134*, 16.
[28] Z. Wang, Z. Hao, X. Zhao, Q. Lin, in *2019 20th Int. Conf. Solid-State Sens., Actuators Microsyst., Eurosens. XXXIII*, IEEE, Piscataway, NJ **2019**, p. 2428.
[29] A. Adumitrachioaie, M. Tertis, M. Suciu, F. Graur, C. Cristea, *Electrochim. Acta* **2019**, *311*, 50.
[30] A. J. Jajack, *Ph.D. Thesis*, University of Cincinnati, **2018**.

[31] B. Zhang, B. Liu, G. Chen, D. Tang, *Biosens. Bioelectron.* **2014**, *53*, 465.
[32] J. Huang, L. Zhao, W. Lei, W. Wen, Y. Wang, T. Bao, H. Xiong, X. Zhuang, S. Wang, *Biosens. Bioelectron.* **2018**, *99*, 28.
[33] S. Weng, M. Chen, C. Zhao, A. Liu, L. Lin, Q. Liu, J. Lin, X. Lin, *Sens. Actuators B* **2013**, *184*, 1.
[34] G. R. Brisson, P. Boisvert, F. Péronnet, H. Perrault, D. Boisvert, J. S. Lafond, *Eur. J. Appl. Physiol. Occup. Physiol.* **1991**, *63*, 269.
[35] M. J. Patterson, S. D. R. Galloway, M. A. Nimmo, *Exp. Physiol.* **2000**, *85*, 869.
[36] C. Huang, Z. Hao, T. Qi, Y. Pan, X. Zhao, *J. Materiomics* **2020**, *6*, 308.
[37] Y. Ohno, K. Maehashi, Y. Yamashiro, K. Matsumoto, *Nano Lett.* **2009**, *9*, 3318.
[38] S. Mao, G. Lu, K. Yu, Z. Bo, J. Chen, *Adv. Mater.* **2010**, *22*, 3521.
[39] C. Wang, Y. Li, Y. Zhu, X. Zhou, Q. Lin, M. He, *Adv. Funct. Mater.* **2016**, *26*, 7668.
[40] N. Tuleuova, C. N. Jones, J. Yan, E. Ramanculov, Y. Yokobayashi, A. Revzin, *Anal. Chem.* **2010**, *82*, 1851.
[41] B. Sahin, M. Alomari, T. Kaya, *Ceram. Int.* **2015**, *41*, 8002.
[42] S. Farid, X. Meshik, M. Choi, S. Mukherjee, Y. Lan, D. Parikh, S. Poduri, U. Baterdene, C. Hung, Y. Wang, P. Burke, M. Dutta, M. A. Stroscio, *Biosens. Bioelectron.* **2015**, *71*, 294.
[43] Y. Chen, T. S. Pui, P. Kongsuphol, K. C. Tang, S. K. Arya, *Biosens. Bioelectron.* **2014**, *53*, 257.
[44] Y. Zhu, Y. Hao, E. A. Aogla, J. Yan, D. Li, K. Xu, Q. Wang, J. Hone, Q. Lin, *Nanoscale* **2016**, *8*, 5815.